A Design for *In-Situ* Measurement of Optical Degradation of High Power Light-Emitting Diodes Under Accelerated Life Test

Quan Chen, Qi Chen, Sheng Liu, and Xiaobing Luo, *Senior Member, IEEE*

***Abstract*—To better understand the reliability problem in high-power light-emitting diodes (LEDs), an online test is critical under an accelerated life test. In this paper, an experimental equipment was proposed for *in situ* measurement to evaluate the degradation of LED's optical properties. Signals such as illuminance and correlated color temperature were transmitted by the heat-resistant optical cable and were finally collected by detectors with high precision. The multichannel outputs were provided to simultaneously measure several samples. The measuring distance optimization was conducted by a ray tracing method, and the characteristics of optical output were listed. Accelerated life tests also indicate that the system error is less than 0.2%, and the measuring uncertainty of equipment can be controlled within 2%. A comparison experiment according to LM-80 measurement standard also shows a good agreement between the experimental data and the reference value.**

***Index Terms*—Light-emitting diodes, *in situ* measurement, accelerated life test.**

I. Introduction

RELIABILITY issues have become a serious bottleneck [1], [2] for widespread application of high-power LEDs. Generally, a test of several thousands hours is required to evaluate product aging properties, while it is very difficult for the manufacturer to do such long time test. So far, the accelerated life test becomes the well known method for reducing the evaluation time effectively [3], and its focus is on finding the characteristics of degradation process at extreme conditions. Commonly used stress parameters under accelerated life test are applied continuously and in cycling.

Manuscript received October 31, 2013; accepted February 17, 2014. Date of publication February 28, 2014; date of current version June 3, 2014. This work was supported in part by the Major State Basic Research Development Program of China under Grant 2011CB013106 and in part by the National Nature Science Foundation of China under Grant 51370670.

Q. Chen is with the School of Electronic and Electrical Engineering, Wuhan Textile University, Wuhan 430073, China, and also with the School of Energy and Power Engineering, Huazhong University of Science and Technology, Wuhan 430074, China.

Q. Chen and X. Luo are with the School of Energy and Power Engineering, Huazhong University of Science and Technology, Wuhan 430074, China (e-mail: Luoxb@hust.edu.cn).

S. Liu is with the School of Power and Mechanical Engineering, Wuhan University, Wuhan 430072, China.

Color versions of one or more of the figures in this paper are available online at http://ieeexplore.ieee.org.

Digital Object Identifier 10.1109/TDMR.2014.2309127

Now optical parameters of LEDs in reliability experiments were mainly measured on basis of off-line testing method [4]–[6]. However, during this process, the test conditions are not controllable in terms of moisture, temperature, time variation and so on. Moreover, the surfaces of LED modules are prone to be stained or scratched when they were moved out from the thermal box to outside for testing, and the light emission characteristics of LEDs may be seriously affected. Therefore, techniques for *in situ* measurement for LEDs should be developed.

Many researches have been provided to measure related parameters of LED optical properties. Bürmen *et al.* [7], [8] developed an automated optical quality inspection system. The intensity, mean color and color variation were obtained for LED reference, the divergence of the optical axis and the viewing angle of the emitting light were measured absolutely. Svilainis [9] presented a technique for LED measurement *in situ*, and the far-field pattern could be measured quickly without dismantling the LEDs from the tile. Zhou *et al.* [10] presented an instrument, which can be used to inspect the quality of LED packaging, and it can simultaneously measure photometric, colorimetric and electrical parameters from the electroluminescence of the LEDs in a matter of millisecond. Chen *et al.* [11] proposed a procedure to adjust the chromaticity coordinates by some engineering statistics methods, and they found that the average value of the color errors can be reduced by constructing an efficient and predictable calibration procedure.

Totally, the speed and precision of the optical detection for LEDs were improved effectively by the above measurement technologies. However, *in situ* measurement in reliability assessment of LEDs is still seldom considered. Particularly, illuminance and correlated color temperature (CCT), as the key parameters of reliability evaluation, should be monitored on real-time.

In this paper, a test method and the prototype for *in situ* measurement of LED optical degradation under reliability test were proposed. The heat-resistant optical fiber was fabricated to convey light to the room temperature circumstance, and a manual assembly fixture was used to provide a good coaxial alignment between the heat-resistant optical fiber and the LED fixture. The partial illuminance and CCT for high-power LEDs were monitored using the specific structure. The optical parameters can be captured continuously via designed system in different reliability testing environments.

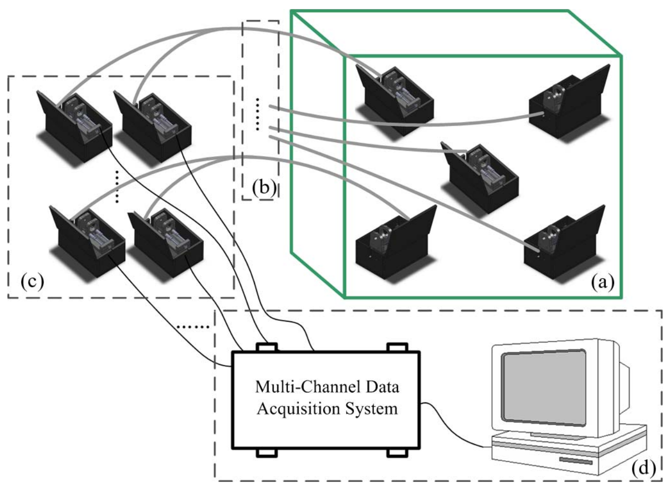

Fig. 1. Configuration of experimental equipment for measuring LEDs optical degradation. (a) Light transmission environment enclosure. (b) Heat-resistant armored cable. (c) Sensing environment enclosure. (d) Photometric and colorimetric measurement system.

II. System Design

Fig. 1 demonstrates the present *in situ* experimental equipment for LEDs aging test. It mainly consists of light transmission environment enclosure, heat-resistant optical cable, sensing environment enclosure, and photometric and colorimetric measurement system. The equipment transmits the partial illuminance and CCT data to a host computer. In order to reflect statistics characteristic of testing sample, five output channels are designed to simultaneously measure various individual sample. The optical parameter data are collected by the standard optoelectronic detectors using digital photoelectric integral method, and it follows the requirement set by CIE127-2007 [12].

During testing, each LED sample is mounted on the light source fixture, which is placed in accelerated life experimental circumstance. LED light emission is transmitted by the heat-resistant armored cable, and is captured by detectors in sensing environment enclosure eventually. The light source and the detector testing fixtures are placed in the light-proof enclosures, respectively, in which some rectangular pores are designed along the inner walls. We use the structure to maintain identical temperature and humidity with external environment. The distance between the tested LEDs and the entrance of optical fiber cable is adjustable to meet different light sources.

Fig. 2 shows the final testing prototype of the present equipment. The armored cable is of Y-type structure, which has the function of single-ended input and double-ended outputs, as shown in Fig. 2(a). A bundle of optical fibers are divided into two parts in quantitative terms. They are butted end-to-end, and are optically aligned by measuring the luminous intensity from one fiber to the other. As for armored cable, the diameters of entrance and exit surfaces are 10 mm and 7 mm, respectively. It is mainly fabricated with the heat-resistant materials and can work with a steady performance from -40 °C to 200 °C. Its characteristics and couple efficiency play a key role for the accuracy of this measurement system. The light outputs from the exit surface of the armored cable are acquired by the detectors of illuminometer and colorimeter, respectively. The spectral responsivity of the photometer is mainly determined by the wavelength-selective $V(\lambda)$ filter, which represents the relative spectral responsivity of human eye under daylight illumination levels. The spectral responsivity is then the product of the spectral responsivity of the photodiode and the spectral transmittance of the $V(\lambda)$ filter [13], which can be calibrated as an entity to account for inter-reflections between the filter and the detector. The filter is in contact with the heat sink, and it is temperature-stabilized, so the detector has a good $V(\lambda)$ match under the room temperature. The detected partial illuminance is proportional to photocurrent, which is modulated to frequency signal with the current-frequency converter (CFC). As for measurement of CCT, its principle is similar to that of the partial illuminance testing. Three independent detectors are provided with different color filters respectively, so that they can match their spectral responses to the curves of CIE-1931 standard.

To obtain good testing data, a manual test fixture is provided for a coaxial optical measurement of light source, entrance and exit surfaces of armored cable and detectors. Fig. 2(b) shows the test fixture, and it is mainly made up of the fixed pedestal, device clamp holder, sliding shaft, cross screws, and helical spring. The distance between light source and entrance surface can be adjusted by cross screws, and the longest distance is decided by the length of the helical spring.

It is found that the measured errors are mainly caused by the small variable displacement. Especially, the stress load on the optical cables and the sensor surfaces can affect test results. The device clamp holder is designed to produce the uniform stress around device when the material is heated or cooled. The heat-resistant bearing is used to reduce relative displacement under the environmental stress.

In this equipment, the optical parameters are collected by the multi-channel data acquisition system, as shown in Fig. 2(c). For each channel, the frequency signal from detector is connected to frequency-to-voltage convert circuit respectively, and its value lies in the range of 1–20 kHz. The frequency signal is the pulse, and is firstly inputted into a single-limit voltage comparator, and then the timing circuit is triggered by the falling edge of the pulse. When the frequency changes, the pulse is differentiated by a R-C network. The average output current is decided by τ. It is called the time constant factor, the value of which is decided by R-C network. To improve the measured accuracy, an operational amplifier provides a buffered output and also acts as a 2-pole filter, and the average current is demodulated as voltage signal. The ripple will be less than 5 mV peak for all frequencies above 1 kHz. A microcontroller unit of STC11F08XE is used to implement multichannel data collection. System test indicates that the shortest sampling time is about 2 seconds when the five channels are operated simultaneously.

The partial illuminance are calculated from the following formula:

$$E_v = f(S) \cdot i \tag{1}$$

where i is the photocurrent, which is caused by the silicon photodiodes inside the detector. $f(S)$ is regarded as the calibration

Fig. 2. Pictures of *in situ* measurement prototype.

function of detector. Since inputting radiant flux has the good linear relationship with photocurrent in the visible region, $f(S)$ can be obtained according to the inverse-square law [14]. By changing the distance between the detector and the standard light source of known luminous intensity, the relationship of illuminance with photocurrent-variation is calibrated. The color is divided into three parameters, which can be calibrated with tri-stimulus theory. The chromaticity coordinates can be measured directly and CCT can be easily obtained.

It is emphasized that the *in situ* measurement equipment must be fixed during the whole testing period. Once tested individuals are substituted, or armored cables are re-installed, the small variable displacement will lead to the large uncertainty, and the test results will be hardly convinced.

III. System Optimization

The optical fiber cable is the key part of the *in situ* measurement system. Its coupling efficiency determines the accuracy of total experimental equipment. When the distance between the tested light source and the entrance surface of armored cable is too far, the flux received by detector will be too tiny to be detected accurately. However, if the distance is too close, LED sample cannot be approximated to an emitting point. In this situation, the light source is considered as an extended emitting area, and the inverse square law can no longer be applied. Therefore, the illuminance and the CCT measured by the detectors are critically dependent on the exact measurement conditions [15]. In addition, the distance between exit surface of armored cable and the detector should also be considered according to the entrance aperture of detector and the beam divergence from the output of the optical cable. In a word, system optimization should be conducted for a good test accuracy.

Optical fiber cable should be idealized for modeling. Fig. 3 shows the optical fiber cable. It is made up of thousands of optical fibers. The optical fibers mainly consist of fiber cores and claddings, and their diameters are 20 um and 50 um, respectively. The numerical aperture (NA) of optical fiber is 0.54 and the receiving angle is 65°. LED chip has a standard size of 1 mm × 1 mm × 0.1 mm, and its radiation power is assumed to be 1 Watt. To simplify numerical model in this system, Y-type optical cable is taken as the single optical fiber

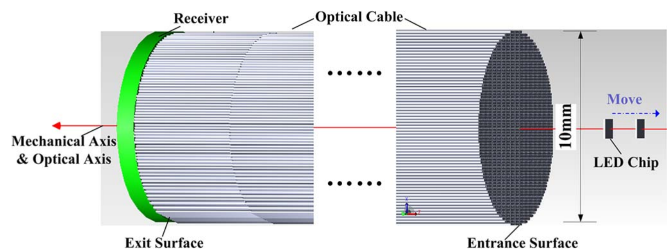

Fig. 3. Distance optimization modeling for LED chip, optical fiber cable, and detector.

cable. The fibers are bundled with the cylindrical package, and the mechanical axis of the package (which is used to match the center of LED chip in the measurement equipment) should coincide with the optical axis (which is the axis of rotational symmetry of the spatial distribution). The distance between the LED chip and the entrance surface of the optical cable is adjusted along the optical axial. The characteristics of the partial flux and the partial average intensity distribution are described in Fig. 4. It can be seen that the increased distance leads to the exponential degradation of the normalized relative flux, but the distribution curve flux is the most approximate to Lambertian emission. Comparing the function of distance-flux and that of distance-intensity distribution, the best position for testing distance is 12 mm.

Because the exit surface and the entrance surface are theoretically perpendicular to optical axis of LED module, the optical fiber cable can be considered as an optical flat with microstructures, and the surfaces are shown in Fig. 5(a). For the rotational symmetry structure of cable, the light extraction of exit surface is theoretically proportional to that of entrance surface. The partial flux are obtained by simulation, as shown in Fig. 5(b). The normalized output is about 2.3123%, and the coupling efficiency of optical fiber cable can be calculated by

$$\eta = \frac{\mathrm{Ev}_{\mathrm{exit}}}{\mathrm{Ev}_{\mathrm{entrance}}} = 50.5\% \tag{2}$$

where $\mathrm{Ev}_{\mathrm{entrance}}$ and $\mathrm{Ev}_{\mathrm{exit}}$ are the illuminances of entrance surface and exit surface, respectively. They are proportional to the flux of entrance surface and exit surface when the received surfaces have the same area.

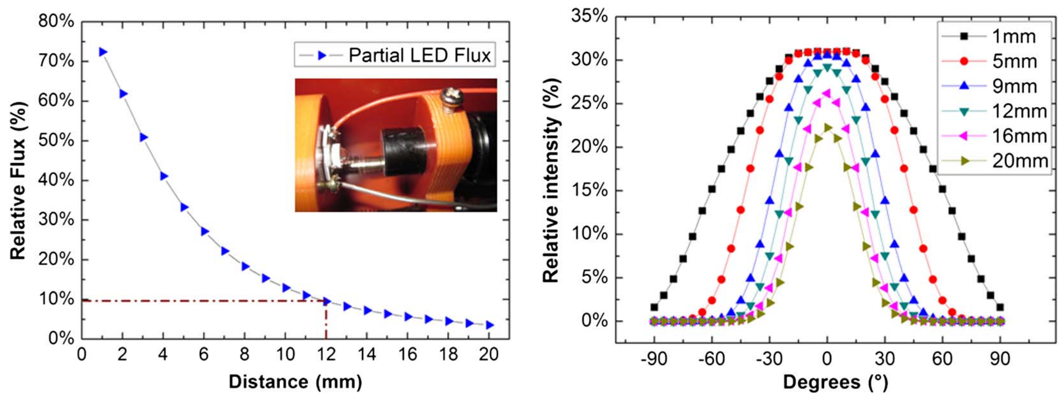

Fig. 4. Normalized partial LED flux and partial intensity distribution of entrance surface in optical fiber cable.

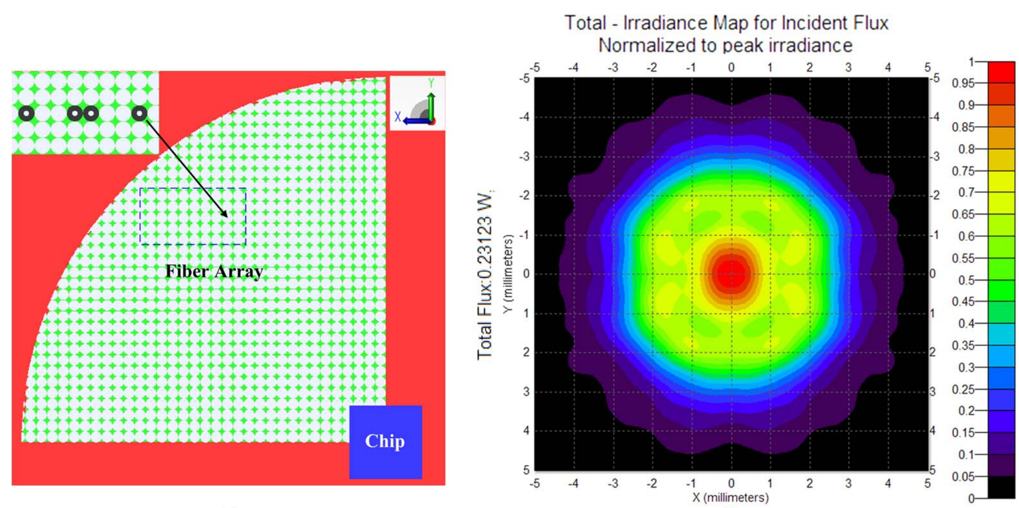

(a) (b)

Fig. 5. Output simulation of optical fiber cable. (a) Composition of optical fiber cable based on microstructures. (b) Illuminance chart of exit surface.

It should be noted that the real area of exit surface in the Y-type optical cable is only half of entrance surface, and the simulation result is based on the hypothesis that the light emitted from exit surface is completely accepted by detector. Therefore, the distance between the detector and the cable can be determined by the numerical aperture of exit surface. Because the divergence angle of exit surface obtained by measurement is about 32°, the most suitable distance is about 5 mm for this system.

IV. Experimental Verification

Four experiments were conducted to evaluate the present *in situ* measurement. Commercial high power blue LED chips were used in the investigation. The peak wavelength is about 456 nm under the rated forward current 350 mA and 1 Watt electrical power. The LED die was soldered on a copper submount and packaged in a conventional way. According to LM-80 measurement standard, LED total flux should be used to evaluate the LEDs lifetimes. To calibrate the relationship between partial illuminance proposed by our equipment and the total flux of the LED die, the sample was operated under various electrical currents, and the total flux was measured by the integrated sphere in the high accuracy array spectral-

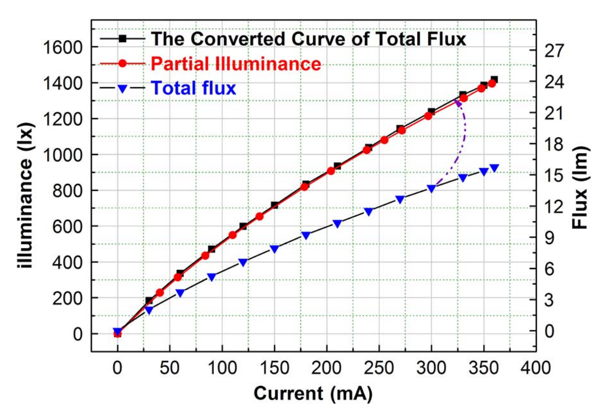

Fig. 6. The relationship between the partial illuminance and the total flux.

radiometer (HAAS-2000, Everfine Ltd.) [16]. The response curves are shown in Fig. 6, as seen from the graph, when the current is 350 mA, tested illuminance is about 1385.1lx, and the total flux is 15.39 lm, the relationship of the two parameters can be represented as

$$\beta = \frac{\phi_t}{\mathrm{Ev}_d} = \frac{\phi_t \cdot S}{\phi_r} \tag{3}$$

where ϕ_t is the total flux, and Ev_d is the measured luminance. ϕ_r is the relative flux, and S is the aperture area of detector.

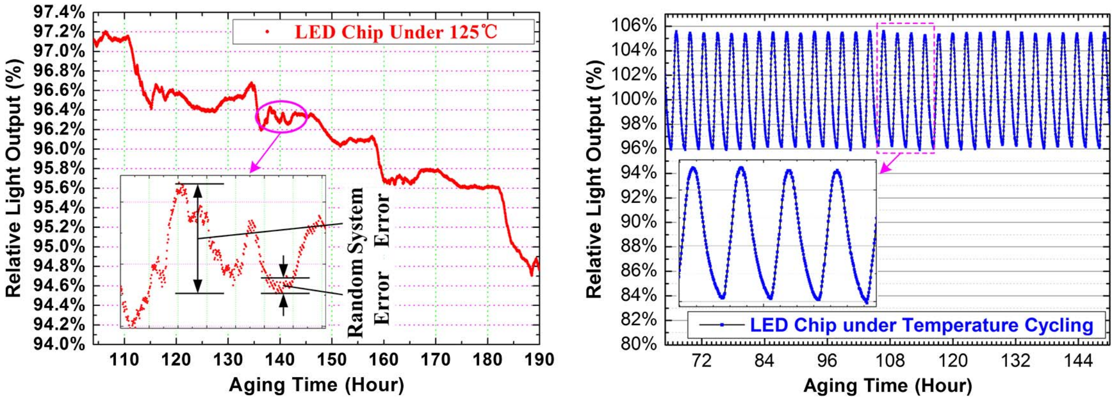

Fig. 7. *In-situ* measurement of the relative light output in high accelerated life test. (a) Optical degradation in constant temperature of 125 °C. (b) Transient response during temperature cycling measurement.

According to the tested data, the transfer coefficient β is a constant, and its value is 0.0111. There is a good linear relationship between the measured illuminance and the total flux. The light output efficiency of system reaches 2.2%. Calculating the maximum deviation under the current of 330 mA, the relative error is up to 1.4%, and the standard deviation is about 0.93%.

In order to analyze the availability of measurement, blue LED modules were placed in the isothermal chamber and operated under the forward current of 350 mA. High accelerated life test was executed with constant temperature of 125 °C, the normalized data of relative illuminance were collected in the specific interval of 30 seconds, as shown in Fig. 7(a). It can be seen that the degradation magnitude of relative illuminance reached 2.5% within about 100 hours. From the chart, it is found that the data of light output has a sudden drop, and in rest of the time, the tested data fluctuate around the certain value. The inset to Fig. 7(a) illustrates that the system error is about 0.2%, and the random error caused by detector is about 0.02%. Fig. 7(b) shows the testing data of temperature cycling life test, where the high temperature side is 125 °C and the low temperature side is −20 °C. The result indicates a good transient response for relative light output with alternating temperature. By selecting the peak and valley of the curve during the aging time from 100 to 150 hours, the measurement uncertainty can be written as

$$\Delta_U = \sqrt{S_{\mathrm{Ev}}^2 + \Delta_S^2} \tag{4}$$

where the standard deviation of S_{Ev} is calculated according to the point of peak value and valley value, which is 1.3%. The system uncertainty Δ_S is regarded as the standard deviation of system. It is easy to get that $\Delta_U = 1.6\%$.

A comparison experiment was operated to discuss the differences of the test results between the present *in situ* measurement and off-line measurement, which followed the LM-80 measurement standard. Ten samples were selected from above commercial white LED modules, and they were measured with 350 mA forward current under the temperature of 55 °C, the initial junction temperature of samples was about 105 °C, the luminous flux data were collected by *in situ* measurement method and by off-line measurement method, respectively. The tested data were averaged and normalized to the initial values

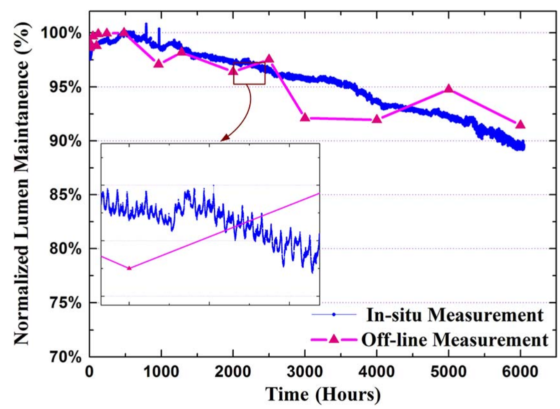

Fig. 8. Comparison of decay curves between *in situ* measurement and off-line measurement according to LM-80 standard.

of the original samples. The lumen maintenance curves during 6000 hours are shown in Fig. 8. It was found that the two curves had the same degrade mode, but the optical depreciation obtained by *in situ* measurement has the better continuity and the smaller measurement uncertainty. Obviously, *in situ* measurement capability with high capture rate is useful for failure mechanism identification.

V. Conclusion

In-situ measurement equipment of LEDs optical degradation under accelerated life test was proposed in this paper. Five output channels were designed to simultaneously measure various individuals. The partial illuminance and CCT for high-power LEDs could be collected continuously by the specific structure. The designed system was verified to have a good agreement with the measurement results by integrating sphere. Confirmatory experiments were conducted in high temperature and cycling test. The distance between the light source and the input interface of heat-resistant optical fiber was optimized, and coupling efficiency of optical sensing was simulated and also calculated by the measurement. Measurement results showed that operation at high levels could induce a significant degradation of the optical characteristics of GaN-based LEDs. The performance of the designed equipment was analyzed, the system error was less than 0.2%, and the measuring uncertainty could be controlled within 2%. Finally, the comparison experiment of 6000 hours indicated the *in situ* measurement can reflect more detailed characteristics for LEDs reliability assessment.

References

[1] S. Liu and X. B. Luo, *LED Packaging for Lighting Applications: Design, Manufacturing, and Testing*. Hoboken, NJ, USA: Wiley, 2011.

[2] M. H. Chang, D. Das, P. V. Varde, and M. Pecht, "Light emitting diodes reliability review," *Microelectron. Reliab.*, vol. 52, no. 5, pp. 762–782, May 2012.

[3] J. Fan, K. C. Yung, and M. Pecht, "Lifetime estimation of high-power white LED using degradation-data-driven method," *IEEE Trans. Device Mater. Rel.*, vol. 12, no. 2, pp. 470–477, Jun. 2012.

[4] J. Z. Hu, L. Q. Yang, and M. W. Shin, "Electrical, optical and thermal degradation of high power GaN/InGaN light-emitting diodes," *J. Phys. D, Appl. Phys.*, vol. 41, no. 3, pp. 035107–035111, Feb. 2008.

[5] G. Meneghsso, M. Meneghini, and E. Zanoni, "Recent results on the degradation of white LEDs for lighting," *J. Phys. D, Appl. Phys.*, vol. 43, no. 45, pp. 354 007-1–354 007-11, Sep. 2010.

[6] S. C. Yang, P. Lin, C. P. Wang, S. B. Huang, C.-L. Chen, P.-F. Chiang, A.-T. Lee, and M.-T. Chu, "Failure and degradation mechanisms of high-power white light emitting diodes," *Microelectron. Reliab.*, vol. 50, no. 7, pp. 959–964, Jul. 2010.

[7] M. Bürmen, F. Pernuš, and B. Likar, "Automated optical quality inspection of light emitting diodes," *Meas. Sci. Technol.*, vol. 17, no. 6, pp. 1372–1378, Jun. 2006.

[8] M. Bürmen, F. Pernuš, and B. Likar, "LED light sources: A survey of quality-affecting factors and methods for their assessment," *Meas. Sci. Technol.*, vol. 19, no. 12, pp. 122 002–122 017, Dec. 2008.

[9] L. Svilainis, "LED directivity measurement *in situ*," *Measurement*, vol. 41, no. 6, pp. 647–654, Jul. 2008.

[10] S. Zhou and S. Liu, "Transient measurement of light-emitting diode characteristic parameters for production lines," *Rev. Sci. Instrum.*, vol. 80, no. 9, pp. 095102-1–095102-7, Sep. 2009.

[11] N. T. Chen and C. W. Chen, "Development of the LED measurement system of chromaticity coordinates correction," *Measurement*, vol. 46, no. 1, pp. 360–366, Jan. 2013.

[12] "Measurement of LEDs," CIE Central Bureau, Vienna, Austria, CIE Tech. Rep. 127-2007, 2007.

[13] G. P. Eppeldauer, "Spectral responsivity-based calibration of photometer and colorimeter standards," *J. Mod. Opt.*, vol. 60, no. 14, pp. 1124–1135, Aug. 2013.

[14] I. Moreno and C. C. Sun, "Modeling the radiation pattern of LEDs," *Opt. Exp.*, vol. 16, no. 3, pp. 1808–1819, Feb. 2008.

[15] "Measurement of LEDs," CIE Central Bureau, Vienna, Austria, CIE Tech. Rep. 127–1997, 1997.

[16] HAAS-2000 high accuracy array spectral-radiometer. [Online]. Available: http://www.everfine.cn

Quan Chen was born in Hubei, China. He received the Ph.D. degree in optoelectronic information engineering from Huazhong University of Science and Technology, Wuhan, China, in 2012. He is currently an Assistant Professor with the School of Electronic and Electrical Engineering, Wuhan Textile University, Wuhan. From September 2012, he has been a Postdoctoral Researcher with the School of Energy and Power Engineering, Huazhong University of Science and Technology, Wuhan.

Qi Chen was born in Hubei, China. He received the B.E. degree in energy and power engineering in 2013 from Huazhong University of Science and Technology, Wuhan, China, where he is currently working toward the Ph.D. degree. His research interest is about high-power LED packaging and reliability.

Sheng Liu received the Ph.D. degree in mechanical engineering from Stanford University, Stanford, CA, USA, in 1992. He has over 21 years of experience in IC and LED packaging. He is currently a specially recruited Professor in Wuhan University, Wuhan, China. His main research interests are LEDs/MEMS/IC packaging, mechanics, and sensors.

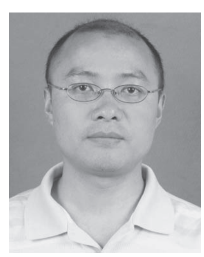

Xiaobing Luo (SM'13) received the Ph.D. degree from Tsinghua University, Beijing, China, in 2002. From 2002 to 2005, he was a Senior Engineer with Samsung Electronics, Suwon, Korea. In September 2005, he became an Associate Professor with Huazhong University of Science and Technology, Wuhan, China, where he has been a Full Professor since 2007 after exceptional promotion. He has published more than 150 papers, including 70 peer-reviewed journal papers and filed more than 40 patents in USA, Korea, and China. His main research interests are LED packaging, heat and mass transfer, and microfluidics devices.